# Field dependence of spin-transfer-induced vortex dynamics in the nonlinear regime

A. Dussaux,[1] A. V. Khvalkovskiy,[1,2,*] P. Bortolotti,[1] J. Grollier,[1] V. Cros,[1,†] and A. Fert[1]

[1]*Unité Mixte de Physique CNRS/Thales and Université Paris Sud, 1 Avenue A. Fresnel, 91767 Palaiseau, France*
[2]*A.M. Prokhorov General Physics Institute of RAS, Vavilova str. 38, 119991 Moscow, Russia*

We derive an analytical model to describe the nonlinear vortex dynamics driven by spin-transfer torque in nanopillar systems. We consider the nonlinearity arising from the magnetostatic and Oersted Zeeman energies. In addition, we determine the linear and nonlinear damping forces through the calculation of the energy dissipation function. Finally, we also consider how the nonlinear dynamics changes with a perpendicular magnetic field that deforms the vortex magnetization profile. The comparison between the analytical model and numerical results obtained from micromagnetic simulations shows an excellent agreement for the change of frequency and amplitude of oscillation of the vortex as a function of the applied current and external perpendicular magnetic field.

## I. INTRODUCTION

The injection of large, spin-polarized currents through magnetic multilayers leads to a number of interesting physical phenomena.[1,2] Termed "spin-transfer torques," the interaction between the spins of charge carriers (e.g., conduction electrons in magnetic metals and holes in dilute magnetic semiconductors) and magnetization leads to additional torques exerted on the magnetization.[3] As a consequence, a number of novel effects, such as magnetization reversal,[4,5] domain-wall propagation in the absence of magnetic fields,[6] and the possibility of self-sustained, large-amplitude magnetization oscillations[7,8] are made possible. The phenomenon of current-driven magnetization oscillations leads to tantalizing possibilities for new nanoscale microwave oscillators[9] for which the frequency can be tunable over a wide range using applied currents and fields or for new microwave detectors.[10,11] The magnetization oscillations in the active layer of a magnetoresistive stack are translated into an electrical signal through the giant- or tunneling-magnetoresistance effect. Since 2003, many experimental and theoretical studies have been initiated to improve the sample characteristics in order to optimize the microwave properties of these nanodevices. Indeed, very promising applications are at stake in the field of telecommunications. While many crucial advances have been made in the fabrication and understanding of such spin-transfer nano-oscillators (STNOs), there remain several critical problems yet to be resolved, in particular, the low microwave power and quality factor of single STNOs. In order to improve these parameters, various solutions have been proposed, such as using magnetic tunnel junctions (MTJs) that should deliver large power[12,13] because of the larger magnetoresistive ratios or synchronizing assemblies of STNOs.[14,15]

An alternative approach to tackle these issues has been recently proposed in which current-driven vortex oscillations are used as the source of microwave power.[16,17] Recently, we demonstrated that large microwave powers and narrow linewidths can be obtained simultaneously by spin-transfer-induced vortex motion in MgO MTJs.[18] Spin-transfer-induced vortex oscillations in nanopillars are model systems to study the effect of a spin-polarized current on the magnetization dynamics. In this objective, a complete description of the influence of a magnetic field or a spin-polarized current on such a gyrotropic mode is therefore necessary to design and predict the actual behavior of any spin-transfer vortex oscillator (STVO). Here we consider the general case of current applied perpendicularly to a disk plane (CPP) with a uniform spin polarizer.

The analytical description of the vortex gyrotropic mode is, in most analytical studies,[19–23] dedicated to the determination of the vortex resonance frequency or the critical current associated with spin-transfer-induced large-amplitude oscillations of the vortex core. These parameters can be calculated by following the Thiele approach, based on the Landau-Lifshitz-Gilbert equation of motion under the assumption of a translational motion for the magnetization distribution of the magnetic vortex state.[24,25]

After introducing the Thiele approach, we give an analytical description of the interaction between the vortex magnetic state and a spin-polarized current (Sec. II). We determine the influence of the Oersted magnetic field on the vortex oscillation frequency and the expression of the different forces induced by the spin-polarized current. In Sec. III we derive the dynamics of the vortex core in the nonlinear regime. We will see that the introduction of two nonlinear restoring forces (linked to both the Oersted-Ampère magnetic field and the magnetostatic energy landscape) and a nonlinear damping force is required. These analytical calculations are then compared to micromagnetic simulations. In Sec. IV we study the vortex oscillation frequency that provides a numerical estimation of the restoring forces and how they change with an external magnetic field. In Sec. V we focus on the oscillation amplitude as a function of field and current that depends on the dissipative forces (spin-transfer forces and damping force). Thanks to these simulations, we will see that our model of the vortex gyrotropic mode in the nonlinear regime gives an excellent agreement with the vortex dynamics observed numerically (Sec. VI). In addition, the last section is dedicated to the variation of the oscillation amplitude as a function of field and current (Sec. VII), which demonstrates that a full and accurate prediction of the microwave power emitted by an STVO is possible.

## II. VORTEX GYROTROPIC MODE
## IN THE LINEAR REGIME

In this section, we recall some of the main points of the classical analytical model for describing the dynamics of a magnetic vortex. Moreover, as our case of interest includes the presence of a spin-polarized current acting on the vortex core, we introduce the influence of the current-induced Oersted-Ampère field on the confinement energy. Then we demonstrate that the energy dissipation function, which is calculated with respect to the rotational motion of the vortex, can be used for a correct analytical expression of the damping force as well as of all possible components of the forces associated with spin-transfer torques, i.e., Slonczewski torque (ST) and field-like-torque (FLT). The derivation of these latter different forces will be important in the next sections of this article to accurately describe the large-amplitude vortex core oscillations due to spin transfer.

In the classical approach,[24,25] the magnetic vortex dynamics is described through the influence of the conservative forces acting on the vortex core position $\mathbf{X}$. The resulting equation, called Thiele's equation, writes in a nanodot of thickness $L$, radius $R$, and saturation magnetization $M_s$ as

$$\mathbf{G} \times \frac{d\mathbf{X}}{dt} - \frac{\partial W(\mathbf{X})}{\partial \mathbf{X}} = 0, \qquad (1)$$

where the gyrovector $\mathbf{G} = -G\mathbf{u}_z$ with $G = 2\pi p L M_s/\gamma$. Here $p$ is the vortex core polarity, $\gamma$ the gyromagnetic ratio, and $W(\mathbf{X})$ is the potential energy of the shifted vortex. Using Eq. (1), it is straightforward to determine the resonance frequency of the vortex gyrotropic mode. Guslienko *et al.*[26] showed that the magnetization distribution of a moving vortex is well described by the two vortices ansatz (TVA),

$$\varphi(\chi, r; \rho, \theta) = \theta + C\frac{\pi}{2} + Arg[re^{i(\chi-\theta)} - \rho]$$
$$+ Arg\left[re^{i(\chi-\theta)} - \frac{R^2}{\rho}\right], \qquad (2)$$

with $\varphi$ the azimuthal angle of the magnetization at any position in the disk plane given by the polar coordinates $(r, \chi)$ [see Fig. 1(a)]. The vortex core position is defined by the polar coordinates $(\rho, \theta)$, where $\rho = |\mathbf{X}|$ is the vortex core shift with respect to the disk center [see Fig. 1(b)], $R$ is the disk radius, and $C = \pm 1$ is the vortex chirality. The TVA satisfies the boundary condition that no magnetostatic charge appear at the
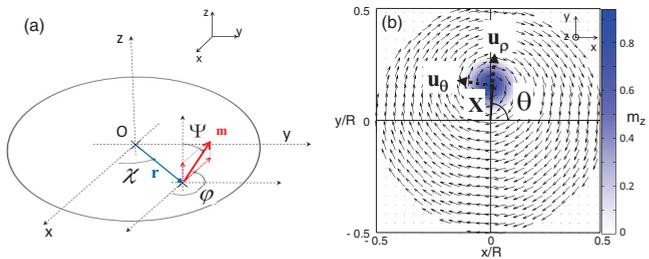
disk border but only in the volume. The variation of the total potential energy associated with a small displacement of the vortex core from the center can be expressed as

$$W(\mathbf{X}) = W(0) + \frac{1}{2}\kappa|\mathbf{X}|^2 + O\left(\frac{|\mathbf{X}|}{R}\right)^4. \qquad (3)$$

Guslienko *et al.*[21] have shown that the variation of the energy $W$ is mainly due to the variation of the magnetostatic energy $W_{ms}$, and the vortex stiffness can be expressed as $\kappa = \kappa_{ms} = \frac{10}{9}\mu_0 M_s^2 \frac{L^2}{R}$.

One of the main goals of this work is to investigate the case of large-amplitude gyrotropic motion of a vortex core induced by spin-transfer torque, which obviously means that a large dc current is injected. Consequently, one needs to consider the influence of the current-induced Oersted-Ampère field.[28] Recently, we calculated[22] this contribution to the total energy by integrating the Zeeman energy $W_{oe}(\mathbf{X}) = \int -\mu_0\mathbf{H}_{Oe}(\mathbf{r})\mathbf{M}(\mathbf{r},\mathbf{X})dV$ on the whole disk. We found that in the presence of a CPP current, the vortex stiffness must be expressed as $\kappa(J) = \kappa_{ms} + \kappa_{oe}J$, with $J$ the current density and $\kappa_{oe} = 0.85C\mu_0 M_s RL$. Here we consider $C = +1$ (−1) for a vortex chirality parallel (antiparallel) to the chirality of the Oersted field induced by a positive current.

The projection of the Thiele equation on the radial and orthoradial axis $(\mathbf{u}_\rho, \mathbf{u}_\theta)$ gives the time variation of the phase $\theta$ and the normalized displacement of the vortex core $s = \rho/R$:

$$\mathbf{u}_\rho : Gs\dot{\theta} - \kappa(J)s = 0, \qquad (4)$$

$$\mathbf{u}_\theta : -G\dot{s} = 0. \qquad (5)$$

From Eq. (4), the resonance frequency of the vortex gyrotropic mode can be expressed as $\omega_0 = \kappa/G = (\kappa_{ms} + \kappa_{oe}J)/G$, valid only for a small oscillation amplitude.

After having considered the conservative forces, hereafter we describe how the dissipative forces that are associated with the damping and the spin-transfer torques act on the vortex core dynamics. It is noteworthy that these forces have been previously calculated in the framework of Thiele's approach.[29] However, we have recently demonstrated that the Thiele approach is not appropriate to give a proper analytical description of the spin-transfer-induced vortex dynamics in a nanopillar because of the assumption of a translational motion of the vortex core.[22] Indeed, a better description is obtained by using the calculation of the energy dissipation and by considering a rotational motion of the vortex core. With this approach, we can give an expression of the different spin-transfer forces acting on a vortex core (see Fig. 2). We first define both the in-plane and out-of-plane components of the forces associated with the ST that, in the case of a uniformly polarized current, writes

$$\mathbf{F}_{ST} = \pi M_s L p_z \sigma J \rho \, \mathbf{u}_\theta + \ln 2 \, \pi M_s L b C \sigma J \mathbf{p}_{x,y}, \qquad (6)$$

where $J$ is the current density, and $p_z$ and $\mathbf{p}_{x,y}$ are the perpendicular and in-plane components of the polarization unit vector $\mathbf{p}$. The spin-transfer torque efficiency is $\sigma = \frac{\hbar P}{2|e|LM_s}$, with $P$ the spin polarization. An important consequence of Eq. (6) is that, in the case of $\mathbf{p}$ and $J$ constant in time and space, a large-amplitude spin-transfer vortex gyration is predicted only if the out-of-plane component of the spin polarization $p_z$



FIG. 1. (Color online) (a) Coordinates of the normalized magnetization $\mathbf{m}$ with a position given by $\mathbf{r}$. (b) Magnetization of an off-centered magnetic vortex in a nanopillar of radius $R$. (arrows) In-plane magnetization given by the TVA [Eq. (2)]. (Color scale) Out-of-plane magnetization given by a Usov ansatz (Ref. 27).
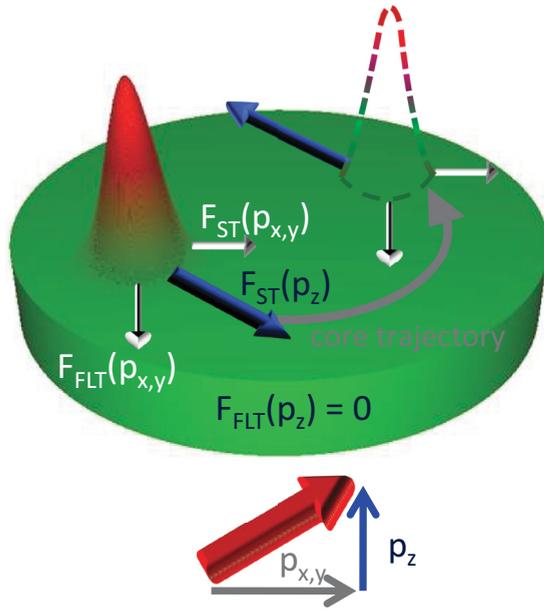
FIG. 2. (Color online) Scheme of the spin-transfer forces acting on a vortex core. The forces are originating from the Slonczewski torque (ST), field-like-torque (FLT), in-plane spin polarization ($p_{x,y}$), and out-of-plane spin polarization ($p_z$).

is different from zero[16] [the first term in Eq. (6)]. In fact, the force induced by the in-plane spin polarization [the second term of Eq. (6)] contributes positively to the energy gain for one semicycle of the vortex motion and negatively for the other semicycle.[30] Now we consider the contributions associated with the field-like-torque (see Fig. 2). This torque is equivalent to the one induced by a magnetic field $\mathbf{H}_{FLT} = -J\,\xi_{FLT}\,\sigma\,\mathbf{p}$, with $\xi_{FLT}$ its relative efficiency with respect to the Slonczewski torque. First, it has to be noticed that the perpendicular spin polarization $p_z$ corresponds to a very small $\mathbf{H}_{FLT}$ (of the order of a few Oersteds at the maximum), which results in a negligible deformation of the vortex shape. The second contribution, which is due to the in-plane spin polarization $\mathbf{F}_{FLT}$, can be expressed as

$$\mathbf{F}_{FLT} = -\frac{dW_{\mathbf{H}_{FLT}}}{d\mathbf{X}} = -C\lambda\pi M_s L R \sigma J \xi_{FLT}(\mathbf{z} \times \mathbf{p}), \quad (7)$$

where $W_{\mathbf{H}_{FLT}}$ is defined by analogy with the Zeeman energy induced by a uniform magnetic field applied in the disk plane.[31] Here, the averaged in-plane magnetization increases with the vortex shift as $\frac{\bar{M}}{M_s} = \lambda(s)s$, at first order $\lambda(s) = 2/3 + O(s^2)$ (see Sec. VII for more details). Similarly to the in-plane contribution for $\mathbf{F}_{ST}$, the force $\mathbf{F}_{FLT}$ can be neglected in the case of a uniform fixed spin polarization because it averages out for a complete gyration of the vortex core.

We now discuss the force induced by the natural damping, which is opposed to the vortex core velocity $\mathbf{F}_D = -D\frac{d\mathbf{X}}{dt}$. For a circular dot,[32] the damping term is written $D = 2\alpha\eta\pi L M_s/\gamma$, where $\alpha$ is the Gilbert damping and $\eta$ is the damping constant. Again, we have used the calculation of the energy dissipation to define $\eta = \ln(R/4l_e) - \frac{1}{4}$, where the exchange length $l_e = \sqrt{2A/\mu_0 M_s^2}$. We notice that this expression of the damping constant is similar to the one derived with Thiele approach[23] $[\eta_{Th} = \frac{1}{2}\ln(R/2l_e) + \frac{5}{8}]$, because the

estimation of the damping torque is less affected by the hypothesis of a translational motion than the spin-transfer torque.

The contributions of the spin-transfer torque and the damping torque on the vortex core dynamics can be added to Eqs. (4) and (5) that become

$$\mathbf{u}_\rho : Gs\dot{\theta} - Ds - \kappa(J)s = 0, \quad (8)$$

$$\mathbf{u}_\theta : -Ds\dot{\theta} - G\dot{s} + a_J Js = 0, \quad (9)$$

with $a_J = \pi M_s L p_z \sigma$ [first term of Eq. (6)]. From Eq. (8), as expected, we obtain that in the linear regime, the stationary ($\dot{s} = 0$) oscillation frequency does not depend on the excitation, $\omega_0 = \kappa/G$. The critical current $J_c$ necessary to obtain sustained vortex oscillations is given by Eq. (9) with ($\dot{s} = 0$),

$$J_c = \frac{D\frac{\kappa_{ms}}{G}}{a_J - D\frac{\kappa_{Oe}}{G}}. \quad (10)$$

An interesting conclusion coming from Eq. (10) is that the critical current $J_c$ depends on the vortex chirality because of the contribution due to the Oersted-Ampère field $\kappa_{oe} = 0.85C\mu_0 M_s RL$. Hence, we predict that for opposite chiralities of the vortex and Oersted field ($C = -1$), the Oersted field confinement $\kappa_{Oe}$ is negative, leading to a smaller $J_c$ compared to the case of similar chiralities $C = +1$.

A major issue is that Eqs. (8) and (9) diverge ($s$ becomes infinite) for $J > J_c$, hence implying that in order to describe analytically the regime of large-amplitude spin-transfer vortex gyration, we must take into account the nonlinear forces acting on the vortex.

## III. ANALYTICAL MODEL IN THE NONLINEAR REGIME

The main objective of the present work is to determine the origin and the influence of all nonlinearities on the vortex core dynamics and therefore be able to describe the variation of oscillation frequency and amplitude as the function of the spin-transfer excitation. We first emphasize that the gyrotropic force Eq. (1) and the effective contribution of the spin-transfer force $\mathbf{F}_{ST}$ [first term of Eq. (6)] calculated from the TVA distribution are perfectly linear with the oscillation amplitude $|\mathbf{X}|$. On the contrary, we must consider the nonlinear contributions for the restoring force and the damping force. Indeed, the potential energy of the shifted vortex and the damping force can be written as a Taylor expansion with respect to $|\mathbf{X}|$. By considering higher-order terms, the potential energy can be expressed as

$$W(\mathbf{X}) = W(0) + \frac{1}{2}\kappa|\mathbf{X}|^2 + \frac{1}{4}\kappa'\frac{|\mathbf{X}|^4}{R^2} + O\left(\frac{|\mathbf{X}|}{R}\right)^6 \quad (11)$$

and the damping as

$$D + D's^2 = \frac{2\pi L M_s}{\gamma}\alpha\eta + \frac{2\pi L M_s}{\gamma}\alpha\eta's^2, \quad (12)$$

where $\eta$ and $\eta'$ are respectively the linear and nonlinear damping constants, and their analytical expressions will be

discussed in Sec. VI. Then we can replace Eqs. (8) and (9) by

$$Gs\dot{\theta} - D(1 + \xi s^2)\dot{s} - \kappa(1 + \zeta s^2)s = 0, \qquad (13)$$

$$-D(1 + \xi s^2)s\dot{\theta} - G\dot{s} + a_J Js = 0, \qquad (14)$$

with $\xi = \frac{\eta'}{\eta}$ the damping nonlinearity factor and $\zeta = \frac{\kappa'}{\kappa}$ the confinement nonlinearity factor. It has to be noticed that the confinement nonlinearity depends on the current again through the Oersted-Ampère field: $\zeta(J) = \frac{\kappa'_{ms} + \kappa'_{oe}J}{\kappa_{ms} + \kappa_{oe}J}$.

Taking into account that $D^2 \ll G^2$ or $(\alpha\eta)^2 \ll 1$ [typically $(\alpha\eta)^2 \approx 10^{-4}$ for NiFe], we obtain that the oscillation frequency is determined solely by the internal energy and does not depend either on the dissipation nor on the spin-transfer excitation [the second term of Eq. (13) is always negligible]:

$$\dot{\theta} = \frac{\kappa}{G}(1 + \zeta s^2), \qquad (15)$$

$$\dot{s} = \frac{D}{G}\frac{\kappa}{G}s[J_{oc} - (\xi + \zeta)s^2]. \qquad (16)$$

We introduce the overcritical current $J_{oc} = \frac{a_J JG}{D\kappa(J)} - 1$. For $J \leqslant J_c$, the term $J_{oc}$ is lower or equal to zero; hence Eqs. (15) and (16) have only one steady solution, $s_0 = 0$ and $\dot{\theta}_0 = \kappa/G$. As expected, the vortex core oscillates at its resonance frequency $\omega_0 = \kappa(J)/G$. For $J > J_c$, the parameter $J_{oc}$ has a nonlinear dependence on $J$ because of the dependence of $\kappa$ on $J$. As a consequence, the previous solutions for $s$ and $\dot{\theta}_0$ become unstable. Thus in the regime of large-amplitude spin-transfer vortex gyration, we obtain the expressions of the oscillation frequency and the amplitude:

$$\omega_{NL} = \omega_0 \left(1 + J_{oc}\frac{\zeta}{\zeta + \xi}\right), \qquad (17)$$

$$s_{NL} = \sqrt{\frac{J_{oc}}{\zeta + \xi}}. \qquad (18)$$

In fact, we notice that the nonlinearity of the confining force due to the magnetostatic energy landscape has been recently calculated using other approaches and leads to a linear increase of the oscillation frequency $\omega_{NL}$ with the current $J$.[23,29,33] However, this prediction does not agree with either experimental results[34] nor numerical simulations.[22] One of the key results of this work is to demonstrate that it is of major importance to also take into account the nonlinearities associated with the Oersted field confining force and to the damping force. Indeed, we can consider two limiting cases for the variation of the oscillation frequency $\omega_{NL}$ with $J$ [see Eq. (17)]. On one hand, for a small nonlinearity of the confinement ($\zeta \ll \xi$), the frequency follows the resonance frequency [$\omega_{NL} = \omega_0(J)$], even with a finite amplitude (see red curves in Fig. 3). As mentioned before, this frequency depends on the vortex chirality with respect to the Oersted-Ampère field chirality, i.e., $\omega_{0+}$ ($\omega_{0-}$) corresponds to parallel (antiparallel) chiralities. On the other hand, for a weak nonlinearity of the damping force ($\zeta \gg \xi$), the frequency is given by the equilibrium between the spin-transfer force and the linear damping force [see Eq. (9)]. Then we derive $\omega = \omega_0(1 + J_{oc}) = \frac{a_J J}{D}$ (see dotted blue line in Fig. 3).

We emphasize that the nonlinear parameters $\zeta$ and $\xi$ have the same order of magnitude. Moreover, for most experiments
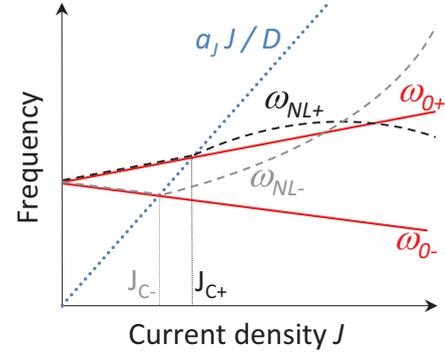


FIG. 3. (Color online) Evolution of the frequency with the current density for the two chiralities. Symbols + and − refer, respectively, to the parallel and antiparallel configurations of the vortex and Oersted field chiralities. Resonance frequency (full red lines). Frequency given by the equilibrium between the spin-transfer force and the linear damping force (dotted blue line). Frequency in the nonlinear regime (dashed lines).

the vortex chirality is forced by the Oersted field chirality. In this case, we find that the frequency $\omega_{NL+}$ can go below the resonance frequency $\omega_{0+}$ for large current densities in the overcritical regime (see black dashed curve in Fig. 3). Such unexpected behavior occurs because the Oersted nonlinear confinement, which is negative, becomes more important than the magnetostatic nonlinear confinement ($\kappa'_{ms} + \kappa'_{Oe}J < 0$). We also predict some interesting features for the opposite case with antiparallel chiralities. Indeed, we find that because the oscillation frequency at a given $J$ is smaller than in the parallel case, it results in a smaller damping and thus in a smaller critical current $J_{c-}$. Moreover, the fact that the Oersted nonlinear confinement and the magnetostatic nonlinear confinement are both positive, and therefore act in the same sense, implies that a large frequency tunability can be achieved (see gray dashed curve in Fig. 3), which can be advantageous for obtaining a more efficient synchronization of several vortex-based oscillators.

## IV. OSCILLATION FREQUENCY / CONFINING FORCES

In this section our purpose is to study numerically the oscillation frequency of the vortex gyrotropic mode and to compare these results with the analytical model presented in Sec. III. The nanopillar system we consider is a stack composed of ferromagnet/spacer/NiFe (free layer) with a diameter of 550 nm. The micromagnetic simulations are performed by numerical integration of the LLG equation using the micromagnetic code SPIN PM based on the fourth-order Runge-Kutta method with an adaptive time-step control for the time integration. We have used a two-dimensional mesh with in-plane cell size of $5 \times 5$ nm$^2$. All the material parameters have been extracted from experimental measurements that will be discussed elsewhere. The NiFe free layer is 4.8 nm thick and has the following magnetic parameters: $M_s = 6.4 \times 10^5$ A/m, $A = 1.3 \times 10^{-11}$ J/m, $\alpha = 0.01$, and $P = 0.3$.

As mentioned in Sec. II, in the case of a uniform spin polarizer, large-amplitude vortex gyrations are predicted only for an out-of-plane component of the spin polarization $p_z$ different from zero. In our previous experimental work, we

obtained a large $p_z$ by applying a large out-of-plane field.[18] As a consequence, hereafter we also consider the influence of a perpendicular magnetic field on the vortex core dynamics. We first recall the analytical expression of the resonance frequency in the absence of current and field:

$$f^{th}(s) = f_0^{th} + f_1^{th} s^2 = \frac{1}{2\pi} \frac{\kappa}{G}(1 + \zeta s^2). \qquad (19)$$

The influence of a perpendicular magnetic field $H_{perp}$ on the resonance gyrotropic frequency has been studied by deLoubens *et al.*[35] When $H_{perp}$ increases, the vortex tail magnetization is no longer constrained in the disk plane. The perpendicular component of the vortex tail magnetization can be written as $m_z = \cos(\Psi_0) = H_{perp}/H_s$, with $\Psi_0$ the colatitude angle of the magnetization and $H_s = 4\pi M_s$ the saturation field. From now on, we will refer to the normalized perpendicular field $h = H_{perp}/H_s$. The confinement constant $\kappa_{ms}(h)$ is calculated by considering that the main contribution to the potential energy variation comes from the dipolar energy of the volume magnetostatic charges created by the in-plane magnetization of the shifted vortex. The vortex core magnetization is neglected and the amplitude of the in-plane component of the vortex tail magnetization is $m_{par} = \sin(\Psi_0)$. The magnetostatic energy goes like the square of the in-plane magnetization gradient and one can deduce $\kappa_{ms}(h) = \kappa_{ms}(0) \sin^2(\Psi_0)$. Moreover, the fact that the magnetization in the vortex tail goes out of plane due to an external perpendicular magnetic field leads to a decrease of the magnetization gradients inside the vortex core. Hence the gyrovector decreases as $G(h) = G(0)[1 - p \cos(\Psi_0)]$, with $p$ the vortex core polarity, and finally the field dependence of the frequency is[35]

$$f_{ms}^{th}(h) = f_{ms}^{th}(0)(1 + p\,h). \qquad (20)$$

The Oersted-Ampère field confinement constant $\kappa_{Oe}$ is given by the scalar product $\mathbf{M}\,\mathbf{H}_{oe}$ that is proportional to the in-plane magnetization $m_{par} = \sin(\Psi_0)$ as the Oersted field $\mathbf{H}_{oe}$ is nonzero only in the disk plane. We obtain that the frequency change associated with the Oersted field evolves as

$$f_{Oe}^{th}(h) = f_{Oe}^{th}(0)(1 + p\,h)(1 - h^2)^{-1/2}. \qquad (21)$$

Note that the Oersted-Ampère field also confines the magnetization of the vortex tail in the layer plane. This feature will be neglected here but can be non-negligible for disks that have a large aspect ratio.

In Fig. 4, we present the simulation results obtained for $h = 0.4$ showing the variation of the frequency with the oscillation amplitude $s$. The frequency has been extracted for two different cases: (i) a small Gilbert damping $\alpha = 0.001$ and no spin transfer (black squares in Fig. 4), and (ii) a spin-transfer torque with $J = 2.5 \times 10^{10}$ A/m$^2$, no damping ($\alpha = 0$), and no Oersted field (see red dots in Fig. 4). We notice that these two curves are perfectly superimposed, a result in agreement with the prediction of our model that the oscillation frequency does not depend on the damping rate.

In Table I, we report the linear and nonlinear contribution to the oscillation frequency obtained with the micromagnetic simulations and analytical calculations in the absence of current for $h = 0$ and $h = 0.4$. For $h = 0$, the theoretical value of the frequency in the linear regime $s \ll 1$ is given by $f_0^{th} = \frac{1}{2\pi} \frac{\kappa_{ms}}{G} = 70$ MHz with[21] $\kappa_{ms} = \frac{10}{9} \mu_0 M_s^2 \frac{L^2}{R}$. The theoretical
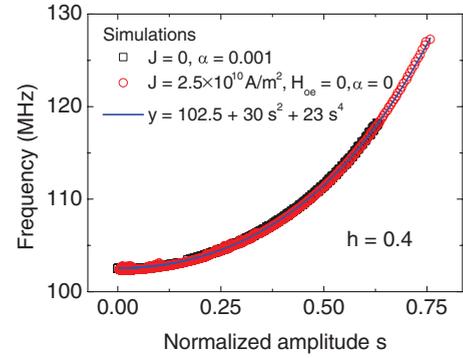


FIG. 4. (Color online) Evolution of the frequency as a function of the oscillation amplitude for $h = 0.4$. Slowly damped oscillations ($\alpha = 10^{-3}$) with no current (black squares). Spin-transfer amplified oscillations with no Oersted field (red dots). Polynomial fit (blue line).

value of the magnetostatic nonlinearity factor is still under discussion.[36] Gaididei *et al.*[33] show that for a non-negligible shift of the vortex core, the resonance frequency evolves as $f^{th} = \frac{1}{2\pi} \frac{\kappa_{ms}}{G} \frac{1}{1-(s/2)^2}$. The first-order Taylor expansion gives $f_1^{th} = 0.25\, f_0^{th}$ (or $\kappa_{ms}' = 0.25\,\kappa_{ms}$), which is in good agreement with our numerical value ($f_1^{sim} = 0.26\, f_0^{sim}$ for $h = 0$). For nanopillars with higher aspect ratios $L/R$, the nonlinear magnetostatic confinement gets smaller. It can even become negative with a disk radius equal to a few exchange lengths.[37]

For $h = 0.4$, the frequency obtained with the micromagnetic simulations remains in good agreement with the theory. According to Eq. (20), $f^{th}$ $(h = 0.4) = 1.40$ $f^{th}(0)$. In the simulation we obtain $f_0^{sim}(h = 0.4) = 1.40$ $f_0^{sim}(0) = 102.5$ MHz for the linear frequency.

According to the calculation of the Zeeman energy due the Oersted-Ampère field, we find that the Oersted nonlinear confining constant is $\kappa_{Oe}' = -0.42 C \mu_0 M_s R L$. In order to define the influence of the Oersted field on the oscillation frequency with the simulations, we vary the current density up to $J = 2.5 \times 10^{10}$ A/m$^2$ and we subtract the frequency $f(s)$ measured without current. With no surprise, the frequency shift induced by the Oersted field is proportional to the current.

The numerical values (see Table II) are in excellent agreement with the values predicted from the analytical model ($f_0^{th} = \kappa_{Oe} J/G$, $f_1^{th} = \kappa_{Oe}' J/G$ for $h = 0$) and from the field influence given by Eq. (21) for $h = 0.4$.

## V. OSCILLATION AMPLITUDE / DISSIPATIVE FORCES

In this section, we focus on the determination of the amplitude of the vortex core gyration that can be induced by

TABLE I. Oscillation frequency obtained with micromagnetic simulations and analytical calculations for $J = 0$ and $h = 0, 0.4$. The linear frequency $f_0$ and the nonlinear frequency shift $f_1$ are defined in Eq. (19).

|  | $h = 0$ | | $h = 0.4$ | |
|---|---|---|---|---|
|  | $f_0$ (MHz) | $f_1$ (MHz) | $f_0$ (MHz) | $f_1$ (MHz) |
| Theory | 70 | 17.5 | 98 | 24.5 |
| Simulations | 73 | 19 | 102.5 | 30 |

TABLE II. Frequency shift induced by the Oersted field with, as an example, $J = 10^{10}$ A/m$^2$. These values increase linearly with $J$. Parameters $f_0$ and $f_1$ are as defined in Eq. (19).

| | $h = 0$ | | $h = 0.4$ | |
|---|---|---|---|---|
| | $f_0$ (MHz) | $f_1$ (MHz) | $f_0$ (MHz) | $f_1$ (MHz) |
| Theory | 13.1 | −6.5 | 20.0 | −9.8 |
| Simulations | 12.3 | −6.4 | 19.3 | −9.5 |

spin-transfer torque. As we already mentioned, the oscillation amplitude $s$ is directly related to the balance between the dissipative forces, i.e., the spin-transfer force and the damping force that are tangent to the vortex core trajectory:

$$\dot{s} = \frac{a_J J}{G} s - \frac{D}{G}(1 + \xi s^2)s\dot{\theta}. \tag{22}$$

Here, our approach is similar to what we have done for the conservative forces in Sec. IV, to perform micromagnetic simulations in order to estimate the amplitude of the dissipative forces and their variation with a perpendicular magnetic field and to compare these numerical results to the prediction of our analytical model.

The energy dissipated by the spin-transfer force and the damping force depends on the oscillation amplitude of the in-plane component of the magnetization. It can be shown that these two forces are proportional to $\sin^2(\Psi_0)$. By adding the field dependence of the gyrovector $G(h) = G(0)[1 - p\cos(\Psi_0)]$, we determine the influence of the perpendicular field on the vortex oscillation amplitude $s$:

$$\frac{D}{G}(h) = \frac{D}{G}(0)(1 + ph), \tag{23}$$

$$\frac{a_J}{G}(h) = \frac{a_J}{G}(0)(1 + ph). \tag{24}$$

Our strategy is again to consider two limiting cases. The first one corresponds to the case for which the dissipative force is only due to the spin-transfer force, i.e., damping parameter $D = 0$. Then the expression of the oscillation amplitude given in Eq. (22) reduces to

$$\dot{s} = \frac{a_J J}{G} s. \tag{25}$$

A time-dependent solution of this equation can be taken as $s(t) = s(0)e^{\frac{a_J J}{G}t}$. In Fig. 5(a) we show the time variation of the oscillation amplitude obtained for an applied field $h = 0.4$ and three current densities: $J = 1.8, 2.1,$ and $2.5 \times 10^{10}$ A/m$^2$. We see that the simulated curve of $s(t)$ can be perfectly fitted by an exponential function (see red curve for $J = 1.8 \times 10^{10}$ A/m$^2$ in Fig. 5), demonstrating that the spin-transfer force nonlinearity is negligible. As presented in Fig. 5(b), the dissipation rate $\frac{a_J J}{G}$ deduced from the exponential fit increases linearly with $J$, as expected for the spin-transfer force. Finally, we obtain an excellent agreement between the numerical and analytical values of $\frac{a_J}{G}$, as shown in Table III. Note that this result provides the evidence that the spin-transfer force calculated through the energy dissipation function and within the TVA approximation is perfectly accurate.

The second limiting case for the estimation of the oscillation amplitude corresponds to the one in which the spin-transfer torque is neglected, i.e., $a_J = 0$. Hence, the oscillation
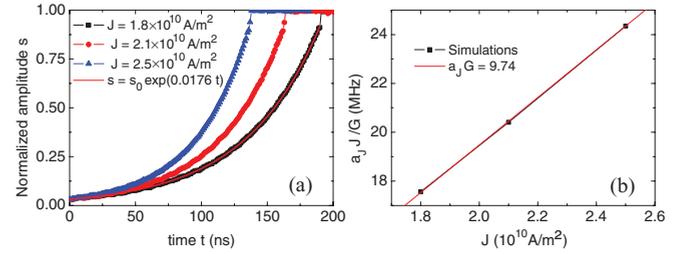


FIG. 5. (Color online) (a) Time variation of the oscillation amplitude amplified by spin transfer at different currents and for $h = 0.4$ (symbols). Exponential adjustment for $J = 1.8 \times 10^{10}$ A/m$^2$ (red curve). (b) Numerical results (black squares), linear adjustment (red line) of the spin-transfer force efficiency as a function of the current density $J$.

amplitude changes are governed by the damping force and Eq. (22) is written

$$\dot{s} = -\frac{D}{G}(1 + \xi s^2)\dot{\theta}s, \tag{26}$$

with the frequency $\dot{\theta}$ that is a function of $s^2$. The solution of $s(t)$ is not trivial. The linear contribution of the damping can be simply extracted, like for the STT term, by using an exponential decrease in the case of small amplitude of the vortex trajectory and we find $\eta^{\text{sim}} = 1.89$ for $h = 0$. Note that the linear damping constant calculated with the energy dissipation function, i.e; $\eta^{th} = \ln(\frac{R}{4l_e}) - \frac{1}{4}$ gives $\eta^{th} = 2.02$ with the vortex core radius $b$ equal to twice the exchange length $l_e$. As for the nonlinear contribution $\eta'^{\text{sim}}$, our approach is to numerically calculate the ratio $\frac{\dot{s}}{\dot{\theta}_s} = \frac{D}{\alpha G} + \frac{D'}{\alpha G}s^2$ that increases with $s^2$. In doing so, we can get a rough estimation that yields $\eta'^{\text{sim}} = 0.73$. Moreover, by introducing higher-order terms is $s$, we can also determine the theoretical value of the nonlinear damping constant $\eta'^{th} = 1/6$. The difference between $\eta'^{\text{sim}}$ and $\eta'^{th}$ comes from the difficulty to evaluate accurately the contribution of the vortex core to the nonlinear damping constant and its dependence on the actual vortex profile.

In order to determine accurately the evolution of the linear damping constant $\eta$ with field, we need to take into account the field dependence of the vortex core radius $b(h)$. This can be obtained from the magnetization distribution [see Fig. 6(a)]. For $h = 0$, we obtain a vortex core size of $b = 17.2$ nm, which has to be compared with the theoretical value $b = 2l_e = 14.2$ nm. Then, when the applied perpendicular magnetic field $h$ increases (in the same direction as the core polarity), the vortex core radius increases [Fig. 6(b)]. The vortex core profile is fitted with a Usov ansatz[27] that we have modified in order to satisfy the condition $m_z = \cos\Psi_0 = h$ in the vortex tail.

TABLE III. Dissipation rate induced by the spin-transfer force obtained with micromagnetic simulations and analytical calculations for $h = 0, 0.4$.

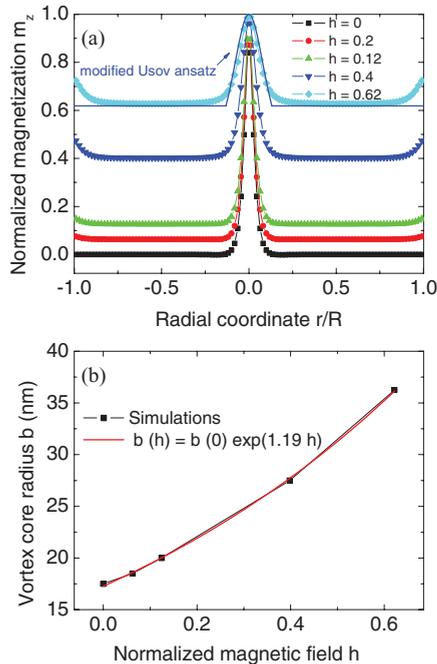| | $\frac{a_J}{G}$ [$10^{-4}$ Hz/(A/m$^2$)] | |
|---|---|---|
| | $h = 0$ | $h = 0.4$ |
| Theory | 6.96 | 9.72 |
| Simulations | 6.90 | 9.74 |

FIG. 6. (Color online) (a) Normalized $m_z$ component of the centered vortex magnetization for different perpendicular magnetic fields $h$ (symbols). Adapted Usov ansatz with $h = 0.4$ (dark blue line). (b) Evolution of the vortex core radius with $h$ (black squares), exponential adjustment (red line).

For $p = +1$, the vortex core perpendicular magnetization is now defined by $\Psi = 2\tan^{-1}[\frac{|r|}{b}\tan(\Psi_0/2)]$ with $\tan(\Psi_0/2) = \frac{\sqrt{1-h^2}}{1+h}$, which can be generalized for any sign of $h$ and $p$ by $m_z = p\frac{b^2(1+p\,h)^2-r^2(1-h^2)}{b^2(1+p\,h)^2+r^2(1-h^2)}$ [see Fig. 6(a) for $h = 0.62$]. Note that in the region outside the vortex core, we find $m_z = h$, which is in good agreement with the numerical results, as already shown by deLoubens *et al.*[35]

We adjust $b(h)$ with an exponential function in order to simplify the expression of $\eta(h)$. The increase of the vortex core size $b(h) = b(0)\,e^{1.19h}$ results in a decrease of the damping constant $\eta^{th}(h) = \eta^{th}(0)\,(1-0.63h)$. In Fig. 7 we show the variation of the ratio $D/(\alpha G)$ calculated from Eq. (23), for which we also take into account the field dependence
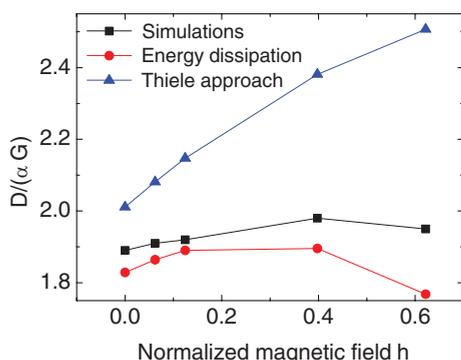


FIG. 7. (Color online) Linear damping $\eta$ as a function of the perpendicular magnetic field $h$: micromagnetic simulations (black squares), calculation of the energy dissipation function (red dots), and Thiele approach (blue triangles).
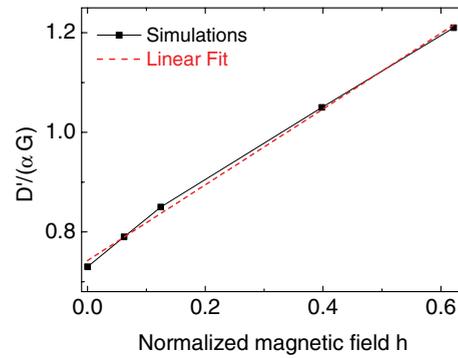


FIG. 8. (Color online) Nonlinear damping as a function of the perpendicular magnetic field $h$: micromagnetic simulations (black squares) and analytical calculations (red dots).

of the vortex core size (red dots). At $h = 0$, the difference between the values for $\eta$ obtained with our approach using the energy dissipation and the Thiele approach (blue triangles) is reasonable. (Note that this conclusion remains valid on a large range of aspect ratios.) On the contrary, as shown in Fig. 7, the field dependence in the simulations indicates that our approach gives a much better agreement for the variation of the damping force than the one predicted by the Thiele approach applied to the case of a nanopillar[23] [$\eta = 0.5\,\ln(\frac{R}{b}) + \frac{5}{8}$]. Finally, we show the field dependence of the numerical values of the ratio $D'/\alpha G$ on Fig. 8. It increases as $(1 + 0.95h)$, which is close to the expected behavior of the damping [see Eq. (23)].

## VI. SPIN-TRANSFER-INDUCED GYROTROPIC MODE

This section includes the most important objective of this work—to achieve a complete description of the spin-transfer-induced vortex dynamics under an external perpendicular field. To reach this goal, we present here the results of micromagnetic simulations of the gyrotropic motion of the vortex core in the overcritical regime that includes both natural damping and spin-transfer torque for $h = 0.4$ parallel to the vortex core. Given our previous results,[18] we know that the perpendicular component of the spin-polarization unit vector is about $p_z = 0.25$. The current density goes up to $J = 2.5 \times 10^{10}$ A/m², and the vortex chirality is parallel to the Oersted field chirality ($C = +1$).

In Fig. 9 we present an important result of this work, that is, the change of both the oscillation frequency $f$ [Fig. 9(a)] and the oscillation amplitude $s$ [Fig. 9(b)] as a function of the current density $J$. We see that the sustained oscillations of the vortex core are observed for currents larger than $J_c = 1.8 \times 10^{10}$ A/m², which is very close to the ones deduced from Eq. (10). Above the threshold value, we find that the oscillation frequency obtained by the simulations increases with $J$ [see black dots in Fig. 9(a)]. Note that the frequency tunability slightly departs from a linear change toward negative values, in agreement with the fact that we consider the case of parallel chirality (see Fig. 3). In order to compare these numerical results with the models, we also plot the oscillation frequency and the oscillation amplitude calculated with Eq. (17) [red curves Fig. 9(a)], taking $J_oc$, $\xi$, and $\zeta$ extracted from simulations. We find a very good agreement
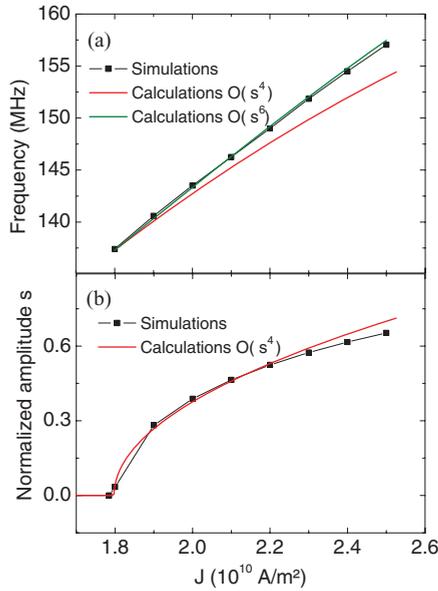
FIG. 9. (Color online) (a) Frequency and (b) oscillation amplitude as a function of the current. Micromagnetic simulations (black squares). (red, green curves) Analytical calculations realized by considering the forces proportional to $s^2$, $s^4$.

between simulations and the analytical model for $J$ slightly above $J_c$. To complete an excellent agreement on the whole current range [see green curve in Fig. 9(a)], we must add a higher order for the nonlinearity of the confinement by using a magnetostatic constant $\kappa''_{ms}$ proportional to $s^6$. This additional term can be calculated by following the method of Gaididei *et al.* for the calculation of the magnetostatic energy.[33] From Fig. 4, we observe that the fourth-order increase of the frequency without Oersted field is given by $f_2^{sim} = 23\, s^4$ MHz for $h = 0.4$. The confinement constant of higher order induced by the Oersted field is thus much smaller and can be neglected.

As far as the oscillation amplitude $s$ is concerned, we see in Fig. 9(b) that the agreement between simulations and the analytical model is already excellent, even when a confinement force proportional to $s^4$ is considered. Even for a large $J = 2.5 \times 10^{10}$ A/m$^2$ we predict a maximum difference of 9%. These results are of major importance because they demonstrate that the spin transfer induced large amplitude gyrotropic motion is very well described by an analytical model taking into account all nonlinearities. In fact, it is a necessary step before going to the description of synchronization between several vortex based spin transfer oscillators.

Finally, in order to probe the potential influence of the spin-transfer torques associated with the in-plane component of magnetization, we perform another set of simulations for which we have added a large in-plane spin polarization $p_x = 0.97$ in addition to the out-of-plane polarization $p_z = 0.25$. We find that even with such a large in-plane polarization, the main features of the vortex dynamics, i.e., frequency and amplitude, are not modified. However, we find that this in-plane component does influence the oscillating behavior as the position of the geometrical center of the oscillations is shifted along $p_x$ due to the Slonczewski torque and along $p_y$ due to the field-like-torque, even if the vortex core trajectory

remains perfectly circular. For $J = 2.5 \times 10^{10}$ A/m$^2$, these two shifts are equivalent ($\approx$5 nm), with $\xi_{FLT} = 0.4$. Note that $F_{FLT}(p_{x,y})$ is a conservative force and thus induces a static shift of the vortex core even without vortex dynamics. This is not the case for the physical mechanism at the origin of the shift due to $F_{ST}(p_{x,y})$. Indeed, this force accelerates or decelerates the vortex core velocity depending on its position in the disk; therefore this phenomena appears only in case of a steady vortex motion. (A recent study also shows that an immobile vortex can be shifted by the Slonczewski torque through the creation of a dip structure.[38])

## VII. OSCILLATOR-EMITTED POWER VERSUS FIELD

In this last section, we want to describe the link between the spin-transfer-induced oscillation amplitude of the vortex core with the oscillating microwave voltage that can be effectively detected using a spectrum analyzer or a high-frequency oscilloscope. In the previous sections, we have determined the influence of the perpendicular field $h$ on the different forces involved in the vortex core dynamics. The resulting microwave power can be expressed as[39]

$$P = \left( \frac{I_{dc}\Delta R_{osc}}{R_s + Z_0} \right)^2 Z_0, \tag{27}$$

where $R_s$ is the sample resistance and $\Delta R_{osc}$ is the amplitude of the resistance oscillation that is proportional to the total magnetoresistance $\Delta R$ and $Z_0$ is the load resistance. In the case of the vortex gyrotropic mode with a uniform in-plane polarizer (that is the most common system), the parameter $\Delta R_{osc}$ is proportional to the normalized in-plane magnetization of the polarizer $m_{x,y}^{pol}$ and of the averaged magnetization oscillation $m_{osc} = \lambda s$ and writes for any external field $h$,

$$\Delta R_{osc} = \lambda s \frac{\Delta R}{2}(1 - |h|)m_{x,y}^{pol}. \tag{28}$$

Note that the parameter $\lambda$ is a function of the vortex core shift $s$. In Fig. 10 we show the change of $\lambda$ with $s$ obtained from micromagnetic simulation and analytical calculations. Indeed, we find that the change of $s_{NL}(h)$ is mainly influenced by the field dependence of the perpendicular spin polarization $p_z = \frac{H_{perp}}{4\pi M_s^{pol}}$, with $M_s^{pol}$ the saturation magnetization of the polarizer. For such a nanopillar system, we know that large-amplitude gyrations of the vortex core can be observed only above a
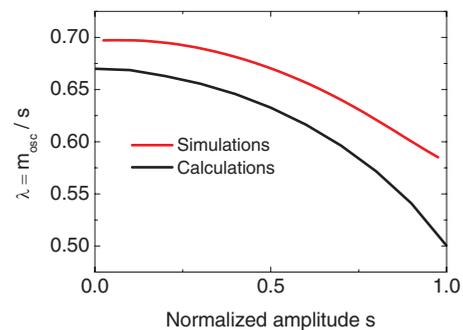


FIG. 10. (Color online) Micromagnetic simulations and analytical calculation of the averaged in-plane magnetization as a function of the vortex core shifts.
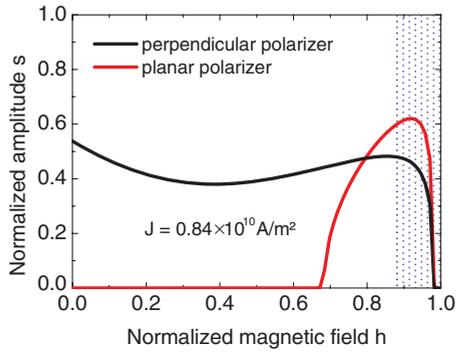
FIG. 11. (Color online) Analytical calculation of the oscillation amplitude as a function of $h$ with $J = 0.84 \times 10^{10}$ A/m$^2$ and a constant perpendicular spin polarization (black squares) or in the case of a constant in-plane spin polarization that results in an effective spin polarization proportional to $h$ (red dots).

threshold field.[18] As a consequence, the maximum of the oscillation amplitude is reached for $h$ close to 1 (see red curve in Fig. 11 with $J = 0.84 \times 10^{10}$ A/m$^2$ and $P\, p_z = 0.2\, h$). However, in this field range the magnetoresistive signal $\Delta R_{\mathrm{osc}}$ goes to 0 and the resulting emitted power can be negligible.

An interesting and nonintuitive result is that, if we now consider a nanopillar system with a perpendicular polarizer (see black curve in Fig. 11 with $P\, p_z = 0.15$), the resulting field dependence of the oscillation amplitude is very weak. (In the blue dotted region the strong deformation of the vortex core makes its analytical description difficult.[41])

Remarkably, a main interest for this structure with perpendicular polarizer is that the best condition[42] to obtain large-amplitude gyration of the vortex core $s_{NL}$ and large oscillation of the resistance $\Delta R_{\mathrm{osc}}$ is achieved in the absence of external field, i.e., $h = 0$. It has to be noticed that even in this simple situation, a stray field induced by the perpendicular polarizer has to be considered, as can be done with our complete analytical description of the vortex gyrotropic mode, taking into account the influence of an external field acting on all forces.

## VIII. CONCLUSION

In summary, we have proposed a thorough analytical description of the spin-transfer-induced vortex dynamics in the nonlinear regime. Moreover, we have carefully treated the influence of an external magnetic field on all forces acting on the vortex core. These derivations are of main importance in order to make our theoretical predictions comparable with the actual configuration for experimental results. In addition to the nonlinear contribution of the confinement due to the magnetostatic energy existing in our nanopillar geometry, we also have introduced an accurate determination of the current-induced Oersted-Ampère forces as well as the nonlinear contributions of the damping forces. We then compared and found excellent agreement between our model and numerical micromagnetic simulations, in the description of the variation of the vortex oscillation frequency and oscillation amplitude under spin-transfer excitation. Moreover, it validates our approach based on the calculation of the energy dissipation that we have developed to give an expression of all the in-plane and out-of-plane components of the spin-transfer forces associated with the Slonczewski term and fieldlike term. The analytical derivation of all these forces represent an important progress to define precisely under which conditions of current and field, large radius vortex core oscillation are predicted. Moreover, our development would allow an analytical description of the phase-locking behavior of a vortex-based oscillator to an external rf signal. This latter analytical modeling is an important step toward optimizing the synchronization efficiency between several vortex-based spin-transfer oscillators.

*Present address: Grandis, Inc., 1123 Cadillac Court, Milpitas, CA 95035, USA.

†Corresponding author: vincent.cros@thalesgroup.com

[1]J. C. Slonczewski, J. Magn. Magn. Mater. **159**, L1 (1996).

[2]L. Berger, Phys. Rev. B **54**, 9353 (1996).

[3]M. D. Stiles and A. Zangwill, Phys. Rev. B **66**, 014407 (2002).

[4]J. A. Katine, F. J. Albert, R. A. Buhrman, E. B. Myers, and D. C. Ralph, Phys. Rev. Lett. **84**, 3149 (2000).

[5]J. Grollier, V. Cros, A. Hamzic, J. M. George, H. Jaffrés, A. Fert, G. Faini, J. Ben Youssef, and H. Legall, Appl. Phys. Lett. **78**, 3663 (2001).

[6]O. Boulle, G. Malinowski, and M. Kläui, Mater. Sci. Eng. R **72**, 159 (2011).

[7]S. I. Kiselev, J. C. Sankey, I. N. Krivorotov, N. C. Emley, R. J. Schoelkopf, R. A. Buhrman, and D. C. Ralph, Nature (London) **425**, 380 (2003).

[8]W. H. Rippard, M. R. Pufall, S. Kaka, S. E. Russek, and T. J. Silva, Phys. Rev. Lett. **92**, 027201 (2004).

[9]J. A. Katine and E. E. Fullerton, J. Magn. Magn. Mater. **320**, 1217 (2008).

[10]A. A. Tulapurkar, Y. Suzuki, A. Fukushima, H. Kubota, H. Maehara, K. Tsunekawa, D. D. Djayaprawira, N. Watanabe, and S. Yuasa, Nature (London) **438**, 339 (2005).

[11]C. Wang, Y.-T. Cui, J. Z. Sun, J. A. Katine, R. A. Buhrman, and D. C. Ralph, Phys. Rev. B **79**, 224416 (2009).

[12]A. M. Deac, A. Fukushima, H. Kubota, H. Maehara, Y. Suzuki, S. Yuasa, Y. Nagamine, K. Tsunekawa, D. D. Djayaprawira, and N. Watanabe, Nat. Phys. **4**, 803 (2008).

[13]B. Georges, J. Grollier, V. Cros, A. Fert, A. Fukushima, H. Kubota, K. Yakushijin, S. Yuasa, and K. Ando, Phys. Rev. B **80**, 060404(R) (2009).

[14] F. B. Mancoff, N. D. Rizzo, B. N. Engel, and S. Tehrani, Nature (London) **437**, 393 (2005).

[15] S. Kaka, M. R. Pufall, W. H. Rippard, T. J. Silva, S. E. Russek, and J. A. Katine, Nature (London) **437**, 389 (2005).

[16] V. S. Pribiag, I. N. Krivorotov, G. D. Fuchs, P. M. Braganca, O. Ozatay, J. C. Sankey, D. C. Ralph, R. A. Buhrman, and N. York, Nat. Phys. **3**, 498 (2007).

[17] Q. Mistral, M. vanKampen, G. Hrkac, J.-V. Kim, T. Devolder, P. Crozat, C. Chappert, L. Lagae, and T. Schrefl, Phys. Rev. Lett. **100**, 257201 (2008).

[18] A. Dussaux, B. Georges, J. Grollier, V. Cros, A. V. Khvalkovskiy, A. Fukushima, M. Konoto, H. Kubota, K. Yakushiji, S. Yuasa *et al.*, Nature Communications **1**, 8 (2010).

[19] K. Y. Guslienko, V. Novosad, Y. Otani, H. Shima, and K. Fukamichi, Appl. Phys. Lett. **78**, 3848 (2001).

[20] C. E. Zaspel, B. A. Ivanov, J. P. Park, and P. A. Crowell, Phys. Rev. B **72**, 024427 (2005).

[21] K. Y. Guslienko, X. F. Han, D. J. Keavney, R. Divan, and S. D. Bader, Phys. Rev. Lett. **96**, 67205 (2006).

[22] A. V. Khvalkovskiy, J. Grollier, A. Dussaux, K. A. Zvezdin, and V. Cros, Phys. Rev. B **80**, 140401(R) (2009).

[23] K. Y. Guslienko, G. R. Aranda, and J. Gonzalez, J. Phys.: Conf. Ser. **292**, 12006 (2011).

[24] A. A. Thiele, Phys. Rev. Lett. **30**, 230 (1973).

[25] D. L. Huber, Phys. Rev. B **26**, 3758 (1982).

[26] K. Y. Guslienko, B. A. Ivanov, V. Novosad, Y. Otani, H. Shima, and K. Fukamichi, J. Appl. Phys. **91**, 7 (2002).

[27] N. A. Usov and S. E. Peschany, J. Magn. Magn. Mater. **118**, L290 (1993).

[28] Y.-S. Choi, S.-K. Kim, K.-S. Lee, and Y.-S. Yu, Appl. Phys. Lett. **93**, 182508 (2008).

[29] B. A. Ivanov and C. E. Zaspel, Phys. Rev. Lett. **99**, 247208 (2007).

[30] A. V. Khvalkovskiy, J. Grollier, N. Locatelli, Y. V. Gorbunov, K. A. Zvezdin, and V. Cros, Appl. Phys. Lett. **96**, 212507 (2010).

[31] K. Y. Guslienko, R. H. Heredero, and O. Chubykalo-Fesenko, Phys. Rev. B **82**, 014402 (2010).

[32] K. Y. Guslienko, Appl. Phys. Lett. **89**, 22510 (2006).

[33] Y. Gaididei, V. P. Kravchuk, and D. D. Sheka, Int. J. Quantum Chem. **110**, 83 (2010).

[34] M. R. Pufall, W. H. Rippard, M. L. Schneider, and S. E. Russek, Phys. Rev. B **75**, 140404(R) (2007).

[35] G. deLoubens, A. Riegler, B. Pigeau, F. Lochner, F. Boust, K. Y. Guslienko, H. Hurdequint, L. W. Molenkamp, G. Schmidt, A. N. Slavin *et al.*, Phys. Rev. Lett. **102**, 177602 (2009).

[36] According to Guslienko *et al.*,[31] the nonlinear magnetostatic confinement $\kappa'_{ms} = 4\kappa_{ms}$ that results in an oscillation frequency multiplied by a factor of 4 when the oscillation amplitude of the vortex core goes close to $R$. This prediction is, however, much larger than our simulation results.

[37] A. Lyberatos, S. Komineas, and N. Papanicolaou, J. Appl. Phys. **109**, 023911 (2011).

[38] V. P. Kravchuk, D. D. Sheka, F. G. Mertens, and Y. Gaididei, J. Phys. D **44**, 285001 (2011).

[39] B. Georges, J. Grollier, V. Cros, and A. Fert, Appl. Phys. Lett. **92**, 232504 (2008).

[40] A. Dussaux, A. V. Khvalkovskiy, J. Grollier, V. Cros, A. Fukushima, M. Konoto, H. Kubota, K. Yakushiji, S. Yuasa, K. Ando *et al.*, Appl. Phys. Lett. **98**, 132506 (2011).

[41] For $h$ close to 1, the ratio $\kappa_{oe}/G$ diverges and $\omega_0$ becomes infinite [see Eq. (21)]. Analytically, it induces a zero-amplitude oscillation. On the contrary, experiments and numerical simulations show a decrease of the frequency in the transition between vortex state and quasiuniform state of the magnetization.[18,40]

[42] For a magnetic field antiparallel to the vortex core ($h < 0$), a decrease of the resonance frequency gives rise to an increase of the oscillation amplitude. Experimentally, it is limited by the polarizer and vortex core switching fields.